

# Evaluation of antibacterial activity using *Aerva lanata* and *Millettia pinnata* leaf extracts mediated ZnO and Cu-doped ZnO nanoparticles

Renuka S.<sup>1</sup>, Hariharan V.<sup>2</sup>, Arulraj J.V.<sup>3</sup>, Sutharsan P.<sup>4</sup>, Gokulakumar B.<sup>5</sup> and Dhanaraj K.<sup>6\*</sup>.

<sup>1</sup>Department of Physics, Government College for Women (A), Kumbakonam - 612 001, Tamilnadu, India

<sup>2</sup>Department of Physics, Rajalakshmi Institute of Technology, Chennai - 600 124, Tamilnadu, India

<sup>3</sup>Department of Biotechnology, Arunai Engineering College, Tiruvannamalai- 606603, Tamilnadu, India,

<sup>4</sup>Department of Physics, Sir Theagaraya College, Chennai-600021, Tamilnadu, India

<sup>5</sup>Department of Physics, Thiru. A. Govindasamy Government Arts College, Tindivanam- 606 603, Tamilnadu, India

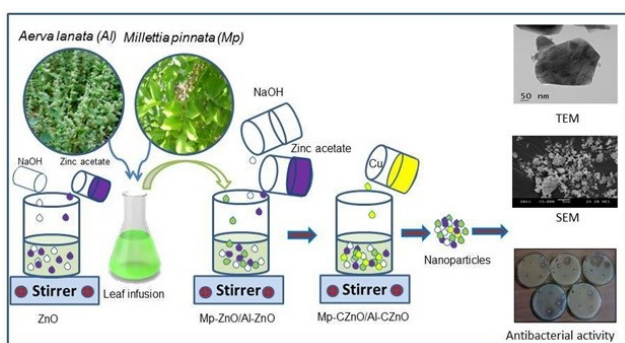
<sup>6</sup>Department of Physics, Arunai Engineering College, Tiruvannamalai - 606 603, Tamilnadu, India

Received: 17/12/2022, Accepted: 14/04/2023, Available online: 25/04/2023

\*to whom all correspondence should be addressed: e-mail: rajidhana01@gmail.com

<https://doi.org/10.30955/gnj.004655>

## Graphical abstract



## Abstract

A green synthesis using a simple precipitation method produced zinc oxide (ZnO), leaf extractions of zinc oxide as *Aerva lanata* (Al-ZnO) and *Millettia pinnata* (Mp-ZnO), copper-doped Al-CZnO and Mp-CZnO nanoparticles (NAPs). They were characterized for their functional group, structural, antibacterial, and luminescence properties. The grown NAPs were examined by Ultraviolet-visible (UV-Vis), Photoluminescence (PL), Fourier Transform-Infrared (FT-IR) spectroscopy, X-ray diffraction (XRD), Scanning Electron Microscopy (SEM), Transmission Electron Microscopy (TEM) and antibacterial activity. The XRD analysis confirms that all NAPs have a hexagonal structure and no impurity phases other than Cu. In consequence of this, Cu ion has been successfully incorporated into the standard ZnO structure. The calculated crystalline size through the XRD pattern of pure ZnO, Al-ZnO, Mp-ZnO, Al-CZnO, and Mp-CZnO NAPs and the average grain size were 81.37, 52.08, 63.24, 37.54, and 30.71 nm, respectively. The optical absorption spectra show that adding Cu reduces the band gap. FTIR is used to assess the functional group and chemical interaction of leaf extraction and Cu-doped ZnO

at various peaks. In addition, its functional groups are observed to correspond to the ZnO bands in all the samples. The microstructure analysis of SEM confirms that all the NAPs are agglomerated by adding the dopant, which turns into a particle-like structure. The antibacterial activity of the NAPs against *Escherichia coli* was measured using the agar well diffusion technique, and the optimum zone of inhibition (ZOI) was found to be 21 mm. Overall, the obtained results revealed that the Mp-CZnO NAPs is a novel and efficient bacterial pathogens present in the aqueous medium. Hence, it is a good representation for future biomedical applications.

**Keywords:** Green synthesis, Cu-doped ZnO, *Aerva lanata*, *Millettia pinnata*, nanoparticles, antibacterial activity

## 1. Introduction

Nanotechnology is a rapidly expanding area that focuses on the fundamental knowledge of the physical, chemical, and biological characteristics of NAPs. At the atomic and subatomic levels, with possible applications in electronics and cosmetics (Raghavendra *et al.*, 2017; Manikprabhu *et al.*, 2014; and Shakeel *et al.*, 2017). ZnO is a versatile semiconducting oxide with extensive applications due to its wide range and direct band gap (3.37 eV at room temperature) semiconductor with a strong cohesive energy of 1.89 eV and large exciton binding energy of 60 meV (Vishnukumar *et al.*, 2018; Jafar *et al.*, 2021). Nanostructures, such as nanowires, nanoarrays, and nanorods, have piqued the interest of researchers over the last decade due to their superior characteristics to bulk materials. NAPs exhibited as excellent crystalline quality, large aspect ratio, and quantum confinement effects (Padmanaban *et al.*, 2021; Jeevanandam *et al.*, 2018). ZnO nanoparticles have become considerably more concentrated as a result of their many uses such as photocatalysis, fuel cells, solar cells, gas sensors, and

antibacterial activity (Tayyab Noman *et al.*, 2021). Prototype ZnO NAPs are extensively utilised as vaccine delivery methods, anti-cancer medications, biomedicine, and as an addition in organic industrial goods (Sharma *et al.*, 2019). It is being given more attention over the years due to its inexpensiveness, nontoxicity, and environmental safety.

ZnO nanoparticles progressiveness and effectiveness may be increased by enhancing and changing their surface area using dopants such as Ag, Fe, Mn, Al, Co, Cr, Pd, and Cu. (Murugadoss *et al.*, 2022; Labhane *et al.*, 2015; Sih-Sian *et al.*, 2019; Shanmugam *et al.*, 2016; Lupan *et al.*, 2011). The optical, magnetic, and electrical characteristics of these transition metals doped with ZnO are improved. Among these, Cu has very high electronic conductivity, absorption changes and other chemical or physical characteristics. It is abundant in the Earth's crust and inexpensive, making it a vital metal for doping (Labhane *et al.*, 2015). Several techniques for producing ZnO and transition metal doped ZnO nanoparticles have been devised. The Cu is a preferred for dopant in ZnO over other transition metals due to its easy overlapping valence band, enhanced electronic and magnetic properties, antibacterial and antioxidant properties, and acceptability for biomedical applications (Manibalan *et al.*, 2021; Ijaz *et al.*, 2017; Shankar *et al.*, 2014). The Cu doped ZnO NAPs have exhibited biological, photocatalytic, optical, and magnetic properties, and the ability to get a lesser particle size compared to ZnO NAPs due to the enhancement of the surface area (Tee *et al.*, 2015; Teng *et al.*, 2016). Murugadoss *et al.*, 2013 has been applied to the optical and structural characterization of CdS/ZnS and CdS:Cu<sup>2+</sup>/ZnS core-shell nanoparticles. In recent years, Murugadoss *et al.*, 2022 has been proposed the construction of novel quaternary nanocomposite and its synergistic effect towards superior photocatalytic and antibacterial application.

At present, material scientists have concentrated on friendly environmental ways for the synthesis and fabrication of NAPs. However, finding a suitable and non-toxic natural compound as well as an eco-friendly solvent solution for green synthesis of metal NAPs is a challenging endeavor (Sankar *et al.*, 2014). Most plants can reduce and capping different metals and metal oxides into NAPs, while certain plants are more capable than the others. These plants play vital roles in the bioreduction, and consequently the formation of NAPs due to their unique phytochemical elements (Safawo *et al.*, 2018). *Millettia pinnata* (L.) belongs to the semi-mangrove plant family, which is an intervenient type between halophytes and glycophytes. It includes a diverse spectrum of physiologically organic substances, including terpenoids, flavonoids, phenols, alkaloids, saponins, and vitamins. *Aerva lanata* (Al) and *Millettia pinnata* (Mp) have been chosen for their useful qualities such as anti-inflammatory, antimicrobial, antidiarrhoeal, antioxidant, antiulcer, antifungal, antilipidoxidative, and antihyperammonemic (Chopade *et al.*, 2008; Baswa *et al.*, 2001; Vetrichevanan *et al.*, 2002; Shirwaikar *et al.*, 2004). Many synthesis methods have been followed by Cu doped ZnO nanoparticles,

including chemical precipitation, microemulsion, hydrothermal, microwave irradiation, sol-gel process, solid-state reaction, sonochemical preparation, and spray pyrolysis methods (Ahmed *et al.*, 2017; Renuka *et al.*, 2017). Among these methods, the chemical precipitation is the most rapid, highly pure, cheap raw materials, easy handling, large scale production, and it is used in industrial applications (Murugadoss, 2014). We are the first report to synthesis of copper doped ZnO from two different leaf extractions. Hence, the present study is aimed to producing cost-effective; ecofriendly Cu doped ZnO NAPs using leaf extraction of *Aerva lanata* (Al) and *Millettia pinnata* (Mp) and to explore its potential antibacterial activity.

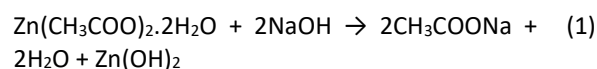
## 2. Materials and methods

### 2.1. Materials

*Aerva lanata* (Al) and *Millettia pinnata* (Mp) (Common name- Sirupeelai and Pungan) leaves were collected from Kumbakonam (31°51'59.3"N, 116°39'34.5"W), Tamilnadu, India. The collected leaves were cleaned twice with running tap water, followed by distilled water. To remove all the dust from the surface of the leaves, the 25 g of sliced leaves were dripping into 250 ml of distilled water and heated at 60°C for 30 min. And then, the infusion was through Whatman40 filter paper to remove all the remains, was stored in refrigerator (4°C) for further analysis. In addition, zinc acetate dihydrate (Zn (CH<sub>3</sub>COO)<sub>2</sub>·2H<sub>2</sub>O), NaOH, copper nitrate hexahydrate (Cu(NO<sub>3</sub>)<sub>2</sub>·6H<sub>2</sub>O), were purchased from Merck.

### 2.2. Synthesis of Zinc Oxide nanocrystals

In the synthesis of ZnO NAPs, 0.6 M of zinc acetate dihydrate was dissolved in 60 ml of deionized water and then stirred vigorously by using a magnetic stirrer. Moreover, 0.2 M of NaOH in 40 ml of deionized water was added drop by drop to the zinc acetate dihydrate solution with vigorous stirring until it forms a white precipitate (Shanmugam *et al.*, 2016; Renuka *et al.*, 2017). The complete reaction of the ZnO synthesis can be expressed as,



The precipitate was collected, and three times washed with distilled water and ethanol. Consequently, the washed precipitate was dried at 100°C for two hours to form the ZnO.



### 2.3. Green synthesis of ZnO nanoparticles

The green synthesis of ZnO nanoparticles by leaf infusion of *Millettia pinnata* (Mp-ZnO) using the method of Ahmed *et al.*, 2017. The 0.6 M of zinc acetate dihydrate was added to 60 ml of distilled water. After 10 min of stirring, 20 ml of leaf infusion of *Aerva lanata* was added drop by drop, followed by 0.2 M NaOH, and the white precipitate was obtained (Al-ZnO). The same procedure has been followed

for the preparation of (Mp-ZnO) NAPs by adding *Millettia pinnata* (Mp) extract with ZnO.

#### 2.4. Green synthesis of Cu-ZnO nanoparticles

By vigorous stirring, zinc acetate dihydrate (0.6 M) was allowed to dissolve in distilled water, and then it was added to 20 ml of leaf infusion of *Aerva Lanata*, followed by 0.2 M of copper nitrate. After 2 hours of stirring (500 rpm) at 80 °C the above solution, 0.2 M NaOH was added drop wise to get white precipitate. Subsequently, the precipitate was washed three times with distilled water and ethanol to dispose of impurities, followed by filtering with Whatman40 filter paper. It was dried at 80 °C in a hot air oven to get the synthesized leaf extract Al-CZnO NAPs. The same procedure has been followed for the preparation of *Millettia pinnata* Cu-ZnO (Mp-CZnO) NAPs. Afterward, these synthesized NAPs were pulverized and stored for future studies.

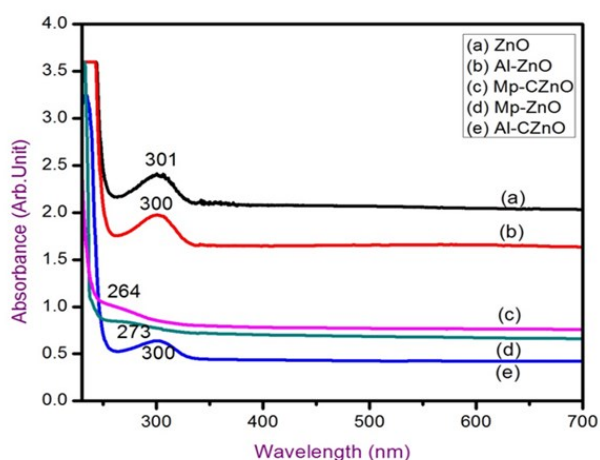


**Figure 1.** UV-Vis analysis result of as synthesized a) ZnO, leaf (*Aerva Lanata*, *Millettia pinnata*) extracted ZnO and Cu doped leaf extracted ZnO

#### 2.5. Antimicrobial activity assay

The antimicrobial activity of the ZnO, Al-ZnO, Mp-ZnO, Al-CZnO and Mp-CZnO NAPs were assessed by a well diffusion method (Suresh kumar *et al.*, 2021). The sterile Muller Hinton agar was flooded into petri dishes for gelatinization. Within 24 hours, the Gram-negative *E. coli* bacterial culture was cultured in nutrient broth. Using a cotton swab, this seed was applied aseptically to the respective agar plates. And then, using a sterile gel puncher, a 6 mm width well was made on the top of the agar plate. The concentration of all the NAPs were taken in the range of 5, 15, 30 and 45 µg/µl were filled into the wells and the plates were incubated at 37 °C for 24 hours. The diameter of inhibition zone was measured and expressed in millimetres (mm).

### 3. Result and discussion

#### 3.1. Optical study

The synthesized NAPs were dispersed in double distilled water, and the absorption properties were analyzed by a UV-Vis spectrophotometer in the range of 200 to 700 nm.

The transitions can occur only for higher photon energies, according to the Fermi exclusion principle, and the shift from the valence band to the conduction band is dependent on the individual dopants. The absorbance wavelengths of all the samples are shown in Figure 1. The absorption peaks recorded for all the samples prepared by ZnO, Al-ZnO (*Aerva lanata*), Mp-ZnO (*Millettia pinnata*) and Cu doped Al-CZnO and Mp-CZnO were 301, 300, 273, 300 and 264 nm respectively. When compared to bulk ZnO, all of the absorption peaks are blue shifted (345 nm) (Murugadoss, 2012). This blue shift indicates the change in band gap along with exciton features, and can be measured by size distribution and particle size is due to the quantum confinement effect (Shanmugam *et al.*, 2016). The band gaps of all the samples were calculated using a simple wave-energy equation,

$$E_g = \frac{hc}{\lambda} eV \quad (3)$$

Where  $h$  is Planck's constant,  $c$  is the light velocity, and  $\lambda$  is the absorption wavelength. The band gaps of ZnO, Al-ZnO, Mp-ZnO, Al-CZnO and Mp-CZnO were about 4.11, 4.13, 4.54, 4.13, and 4.69 eV respectively.

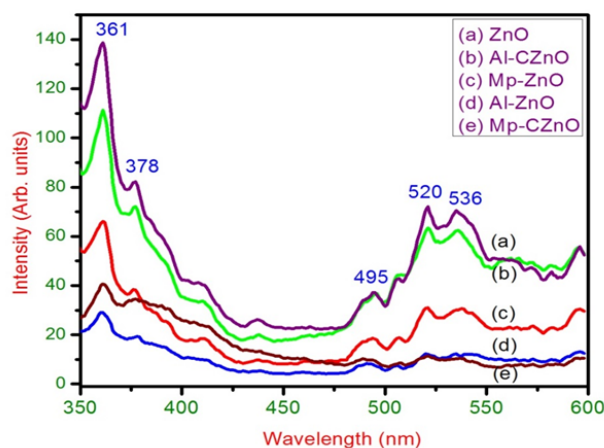


**Figure 2.** Photoluminescence spectra as synthesized a) ZnO, leaf (*Aerva Lanata*, *Millettia pinnata*) extracted ZnO and Cu doped leaf extracted ZnO

The PL spectrum shows (Figure 2) a very strong UV emission peak at 361 nm (3.40 eV), which corresponds to the near band edge emission of ZnO. The significant broad visible emission band was found between 495 and 536 nm (2.50–2.31 eV), and it was linked to the shift between the electron near the conduction band and the hole at the vacancy associated with surface imperfections (Zhang *et al.*, 2010).

#### 3.2. X-ray diffraction analysis

Figure 3 represents XRD patterns of un-doped ZnO, Al-ZnO, Mp-ZnO, Al-CZnO and Mp-CZnO synthesized NAPs. The Bragg's reflection peaks are at 31.62°, 34.88°, 36.50°, 39.34°, 47.24°, 57.24°, 63.85°, 66.26° and 69.27° which correspond to the hexagonal ZnO lattice planes at (100), (002), (101), (102), (110), (103) and (200) respectively. The JCPDS Card No.: 00-001-1136 ZnO hexagonal (wurtzite)

structure was used as a standard to identify the lattice planes depending on the XRD peaks, which demonstrated considerable agreement. The incorporation of Cu into the aforementioned structure shows a minor intensity and peak broadening changes, which shows that the Cu is incorporated in the ZnO structure. There were no impurities or diffraction peaks observed, revealing that just ZnO was present. The average size of the un-doped ZnO and Cu doped ZnO NAPs were derived from the three maximum intense peaks using Debye-Scherrer's formula (Dhanaraj, Suresh, 2018).

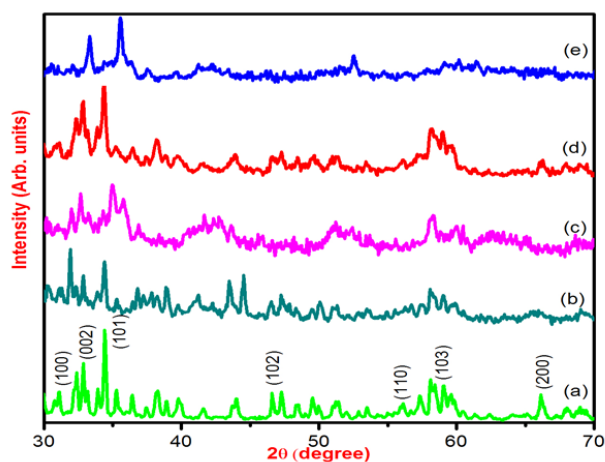


**Figure 3.** XRD patterns of a) ZnO, b) Al-ZnO c) Mp-ZnO, d) Al-CZnO, and e) Mp-CZnO.

$$D = \frac{K\lambda}{\beta \cos \theta} \quad (4)$$

Where, D- particle size in nm,  $\lambda$ - X-ray wavelength,  $\beta$ - FWHM,  $\theta$ - Bragg's angle of reflection. The average size of the synthesized nanoparticles ZnO, Al-ZnO, Mp-ZnO, Al-CZnO and Mp-CZnO were found to be 81.37, 63.24, 52.08, 37.54 and 30.71 nm respectively.

### 3.3. Functional group analysis

The FTIR spectra of un-doped ZnO and Cu-doped ZnO NAPs are shown in Figure 4. Plant extract biomolecules embedded in NAP surfaces were discovered to be responsible for biological activities. Metal oxides normally show absorption bands in the fingerprint region (within  $1000 \text{ cm}^{-1}$ ), which are due to inter-atomic vibrations. The present study of FTIR spectra (Figure 4a) confirmed that the stretching mode ZnO absorption band was between  $500$  to  $590 \text{ cm}^{-1}$ . The probability of a metal-oxide bond corresponds to the hexagonal ZnO wurtzite structure. The fundamental mode of absorption at  $3434 \text{ cm}^{-1}$  corresponds to the asymmetric and symmetric stretching H-O-H vibration, which is due to the bending vibrations of chemisorbed water (Handago *et al.*, 2019). The absorption occurring at about  $1635 \text{ cm}^{-1}$  was due to the aromatic C=C ring stretching, although the high-intensity peak at  $1387 \text{ cm}^{-1}$  was due to the  $-\text{CH}_2$  bending mode of aldehydes and ketones. The vibration bands observed at  $1006$  and  $880 \text{ cm}^{-1}$  were due to the presence of stretching and bending

of C-O and C-H, respectively. The bands  $3000 - 3650 \text{ cm}^{-1}$  are due to the adjustable dissociative absorption of hydrogen on zinc along with the oxide site. There were no additional distinctive peaks in the spectrum (Figures 4b and 4d) that indicate the presence of biomolecules and polyphenols from plant extracts (Mp and Al) in the prepared NAPs through chemisorbed formation. From Figures 4c and 4e, Cu-doped plant extracts ZnO show that there are more characteristic peaks associated with polyphenols and biomolecules. The additional two bands in the spectra were  $1109 \text{ cm}^{-1}$  (C-N) and  $2431 \text{ cm}^{-1}$  (C-H) stretching, which are due to the incorporation of Cu in the Zinc Oxide lattice (Ma *et al.*, 2014).

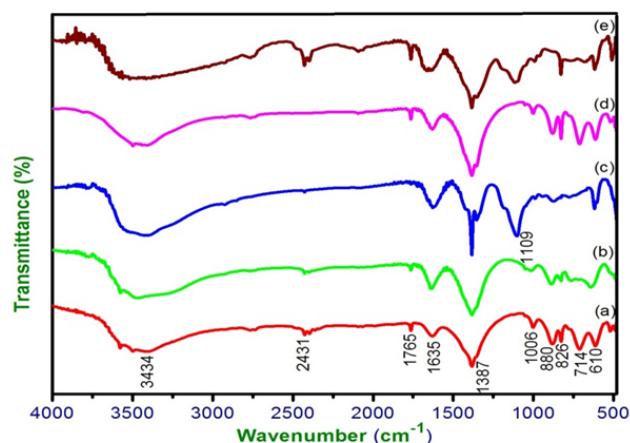


**Figure 4.** FT-IR spectra of a) ZnO, b) Al-ZnO c) Mp-ZnO, d) Al-CZnO, and e) Mp-CZnO.

### 3.4. Morphological analysis

The micrographs of the ZnO, plant extract ZnO, and plant extract Cu-ZnO NAPs, which were deliberated by SEM, are shown in Figure 5 (a-e). It clearly shows that the particles are homogeneous and equally distributed above the surface of NAPs. On the other hand, Figure 5 (a-c) shows that the agglomerated particles and the addition of Cu to ZnO show dispersed (Figure 5 e-f) particles. The SEM measurements showed that the nanoparticles had an average size of less than  $100 \text{ nm}$ , which was in accord with the XRD findings. The TEM images of Al-CZnO and Mp-CZnO are shown in Figure 6, and the Al-CZnO NAPs were agglomerated and had a poorly defined structure. In Mp-CZnO, the particles are clearly distinct and have not aggregated which indicates complete nucleation growth and is well in accordance with the SEM result.

### 3.5. Antibacterial activity

An agar-well diffusion test was used in the current study to assess the antibacterial characteristics of all the substances against the bacterial strain *E. coli* (Dhanaraj *et al.*, 2021; Suresh Kumar *et al.*, 2021). The results are illustrated in Figure 7. The initial line of defence may be harmed as a result of the NAPs' direct interaction with the bacterial cell wall or membrane, which releases metal ions that alter cell

permeability (Gupta *et al.*, 2018). From the zone of inhibition, Mp-CZnO NAPs have the ability to control microorganisms. Among these discoveries, Mp-CZnO (45 g/l) has a significant antibacterial effect against *E. coli* (Table 1). This observation is consistent with recent research by Dobrucka *et al.* (2018), and it suggests that Gram-negative bacteria may be more resistant to antibiotics if they have an outer membrane. Furthermore, Mp-CZnO is to be used for biomedical applications.

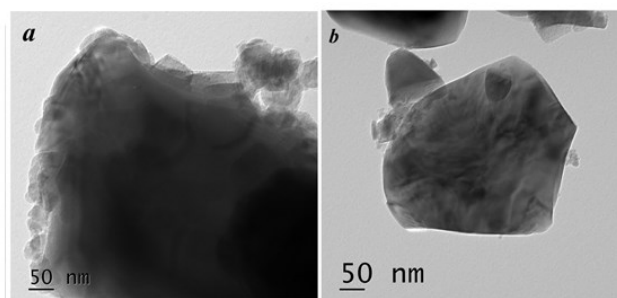


Figure 6. TEM images a) Al-CZnO and b) Mp-CZnO.

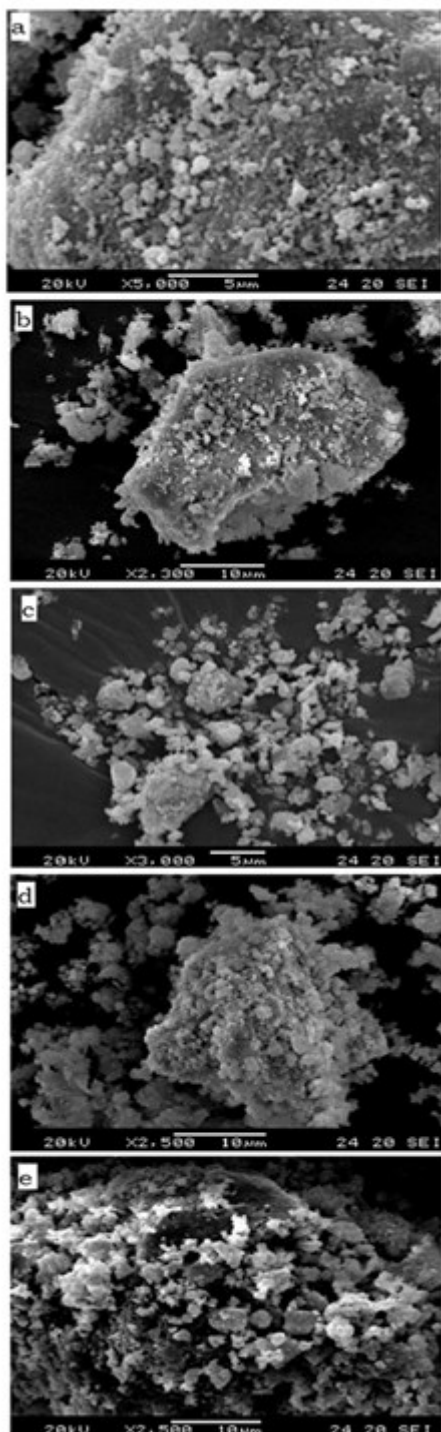


Figure 5. SEM images of a) ZnO, b) Al-ZnO c) Mp-ZnO, d) Al-CZnO, and e) Mp-CZnO

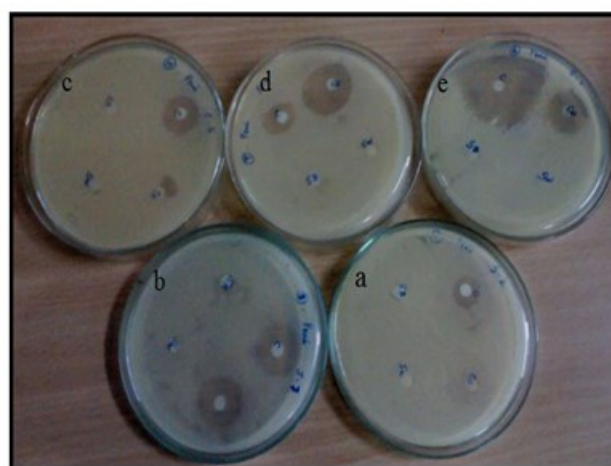


Figure 7. The effect of antibacterial activity with different (5, 15, 30 and 45  $\mu\text{g}/\mu\text{l}$ ) concentration on the *E. coli* for a) ZnO, b) Al-ZnO c) Mp-ZnO, d) Al-CZnO, and e) Mp-CZnO.

Table 1. Antibacterial activity of ZnO, Al-ZnO, Mp-ZnO, Al-CZnO, Mp-CZnO NAPs.

Sample ID	Zone of inhibition (mm)			
	5 $\mu\text{g}/\mu\text{l}$	15 $\mu\text{g}/\mu\text{l}$	30 $\mu\text{g}/\mu\text{l}$	45 $\mu\text{g}/\mu\text{l}$
ZnO	0	0	0	8
Al-ZnO	0	0	10	12
Mp-ZnO	0	0	10	9
Al-CZnO	0	0	8	15
Mp-CZnO	0	0	13	21

#### 4. Conclusion

The synthesis of Cu doped ZnO NAPs with two different leaf extracts (*Aerva lanata* and *Millettia pinnata*), which function as an effective, reducing, and stabilizing capping agent, was achieved by the simple precipitation method. The prepared Mp-CZnO NAPs had a large surface area compared to ZnO NAPs. The UV-Vis and photoluminescence studies express that excitation at 264 nm and emission at 536 nm confirms the defect in ZnO NAPs. The XRD results confirm that the ZnO NAPs have a hexagonal wurtzite structure, and the optimum NAPs size is 37.54 nm for Mp-CZnO. The microstructure analysis showed that leaf extract had an impact on the form and morphology of the particles, causing the agglomerated particles to resemble dispersed particles. The antibacterial studies of the synthesized composite materials revealed the synergistic effect of leaf-extracted Mp-CZnO NAPs on the gram-negative *E. coli*, which has been well established.

The green synthesis of ZnO NAPs forms particle structures, and the leaf extract may enhance their performance. Overall, the present work reported a green, ecofriendly, high yield, and cost-effective method. In the future, leaf-extracted Mp-CZnO can be explored as an antibacterial agent, which will have an extensive range of biomedical applications in various fields.

## References

- Ahmed S., Annu S., Chaudhry A. and Ikram S. (2017). A review on biogenic synthesis of ZnO nanoparticles using plant extracts and microbes: A prospect towards green chemistry. *Journal of Photochemistry and Photobiology B: Biology*, **166**, 272–284.
- Baswa C.C., Rath S.K., Dash R.K. and Mishra R. (2001). Antibacterial activity of Karanj (*Pongamia pinnata*) and Neem (*Azadirachta indica*) seed oil: a preliminary report. *Microbios*, **435**, 183–9.
- Chopade V.V., Tankar A.N., Pande V.V., Tekade A.R., Gowekar N.M., Bhandari S.R. and Khandake R. (2008). *Pongamia pinnata*: Phytochemical constituents, Traditional uses and Pharmacological properties: A review. *International Journal of Green Pharmacy*, **2**, 72–75.
- Dhanaraj K. and Suresh G. (2018). Conversion of waste seashell (*Anadara granosa*) into valuable nanohydroxyapatite (nHAp) for biomedical applications. *Vacuum*, **152**, 222–230.
- Dhanaraj K., Suresh kumar C., Vimalathithan R.M., Socrates S.H., Vinoth Arulraj J. and Suresh G. (2021). A Comparative analysis of microwave assisted natural (*Murex Virgineus* shell) and chemical nanohydroxyapatite: Structural, Morphological and Biological studies. *Journal of Australian Ceramic Society*. **57**, 173–183.
- Dobrucka R., Dlugaszewska J. and Kaczmarek M. (2017). Cytotoxic and antimicrobial effects of biosynthesized ZnO nanoparticles using of *Chelidonium majus* extract. *Biomedical Microdevices*, **20**, 1–5
- Gupta M., Tomar R.S., Kaushik S., Mishra R.K. and Sharma D. (2018). Effective Antimicrobial Activity of Green ZnO Nano Particles of *Catharanthus roseus*. *Frontiers in Microbiology*, **9**, 1–13.
- Handago D.T., Zereffa E.M. and Gonfa B.A. (2019). Effects of *Azadirachta Indica* Leaf Extract, Capping Agents, on the Synthesis of Pure and Cu Doped ZnO-Nanoparticles: A Green Approach and Microbial Activity. *Open Chemistry*, **17**, 246–253.
- Ijaz F., Shahid S., Khan S.A., Ahmad W. and Zaman S. (2017). Green synthesis of copper oxide nanoparticles using *Abutilon indicum* leaf extract: Antimicrobial, antioxidant and photocatalytic dye degradation activities. *Tropical Journal of Pharmaceutical Research*, **16**, 743–753.
- Jeevanandam J., Barhoum A., Chan Y.S., Dufresne A. and Danquah M.K. (2018). Review on nanoparticles and nano-structured materials: history, sources, toxicity and regulations. *Beilstein journal of nanotechnology*, **9**, 1050–1074.
- Jafar Ali Ibrahim S., Rajasekar S., Varsha Karunakaran M., Kasirajan K., Kalyan Chakravarthy N.S., Kumar V. and Kaur K.J. (2021). Recent advances in performance and effect of Zr doping with ZnO thin film sensor in ammonia vapour sensing. *Global NEST Journal*, **23**(4), 526–531.
- Labhane P., Huse V., Patle L., Chaudhari A. and Sonawane G. (2015). Synthesis of Cu Doped ZnO Nanoparticles: Crystallographic, Optical, FTIR, Morphological and Photocatalytic Study. *Journal of Materials Science and Chemical Engineering*, **3**, 39–51.
- Lupan O., Pauporte T., Viana B. and Aschehoug P. (2011). Electrodeposition of Cu-doped ZnO nanowire arrays and heterojunction formation with p-GaN for color tunable light emitting diode applications. *Electrochimica Acta*, **56**, 10543–10549.
- Ma G., Liang X., Li L., Qiao R., Jiang D., Ding Y. and Chen H. (2014). Cu-doped zinc oxide and its polythiophene composites: Preparation and antibacterial properties. *Chemosphere*, **100**, 146–151.
- Manibalan G., Rajesh Kumar M., Murugadoss G., Yesuraj J., Mohan Kumar R., Jayavel R. (2021). Novel chemical route for synthesis of CeO<sub>2</sub>-ZnO nanocomposite towards high electrochemical supercapacitor application. *Journal of Materials Science: Materials in Electronics*, **32**, 8746–8755.
- Manikprabhu D. and Lingappa K. (2014). Synthesis of silver nanoparticles using *Streptomyces coelicolor* kmp33 pigment: an antimicrobial agent against extended spectrum betalactamase (ESBL) producing *Escherichia coli*. *Materials Science & Engineering C*, **45**, 434–437.
- Murugadoss G., Thiruppathi K., Venkatesh N., Hazra S., Mohankumar A., Thiruppathi G., Rajesh Kumar M., Sundararaj P., Rajabathar J.R. and Sakthivel P. (2022). Construction of novel quaternary nanocomposite and its synergistic effect towards superior photocatalytic and antibacterial application. *Journal of Environmental Chemical Engineering*, **10**(1), 106961–68.
- Murugadoss G., Govindarajan D., Zaporotskova I., Kandhasamy N., Rajesh Kumar M. and Kheawhom S. (2022). Enhanced electrochemical and photocatalytic performance of high-quality silver nanoparticles. *Inorganic Chemistry Communications*, **146**, 110162–70.
- Murugadoss G. (2013). Synthesis and photoluminescence properties of zinc sulfide nanoparticles doped with copper using effective surfactants. *Particuology*, **11**, 566–573.
- Murugadoss G. (2012). Structural and optical properties of monodispersed ZnS/CdS/ZnO and ZnO/ZnS/CdS nanoparticles. *Journal of Luminescence*, **132**, 2665–2669.
- Padmanaban A., Murugadoss G., Venkatesh N., Hazra S., Rajesh Kumar M., Tamilselvi R. and Sakthivel P. (2021). Electrochemical determination of harmful catechol and rapid decolorization of textile dyes using ceria and tin doped ZnO nanoparticles. *Journal of Environmental Chemical Engineering*, **9**, 105976–85.
- Raghavendra M., Yatish K.V. and Lalithamba H.S. (2017). Plant-mediated green synthesis of ZnO nanoparticles using *Garcinia gummi-gutta* seed extract: Photoluminescence, screening of their catalytic activity in antioxidant, formulation and biodiesel production. *European Physical Journal - Plus*, **132**, 358–360.
- Renuka S., Dhanaraj K., Socrates S.H. and Gokulakumar B. (2017). Synthesis and characterization of Surfactant (PVP) Capped Zinc Oxide Nanorods. *Elixir Applied Chemical*, **103**, 45678–45681.
- Safawo T., Sandeep B.V., Sudhakar P. and Tadesse A. (2018). Synthesis and characterization of zinc oxide nanoparticles using tuber extract of anchote (*Coccinia abyssinica* (Lam.) Cong.) for antimicrobial and antioxidant activity assessment. *OpenNano*, **3**, 56–63.
- Sankar R., Manikandan P., Malarvizhi V., Fathima T., Shivashangari K.S. and Ravikumar V. (2014). Green synthesis of colloidal

- copper oxide nanoparticles using *Carica papaya* and its application in photocatalytic dye degradation. *Spectrochimica Acta Part A: Molecular and Biomolecular Spectroscopy*, **121**, 746–750.
- Shakeel A.K., Farah N., Sadia K., Ahsan I. and Ghulam H. (2018). Green synthesis of ZnO and Cu-doped ZnO nanoparticles from leaf extracts of *Abutilon indicum*, *Clerodendrum infortunatum*, *Clerodendrum inerme* and investigation of their biological and photocatalytic activities. *Materials science & engineering C, Materials for biological applications*, **82**, 46–59.
- Shanmugam N., Dhanaraj K., Viruthagiri G., Balamurugan K. and Deivam K. (2016). Synthesis and characterization of surfactant assisted Mn<sup>2+</sup> doped ZnO nanocrystals. *Arabian Journal of Chemistry*, **9**, S758–S764.
- Sharma P., Jang N.Y., Lee J.W., Park B.C., Kim Y.K. and Cho N.H. (2019). Application of ZnO-Based Nanocomposites for Vaccines and Cancer Immunotherapy. *Pharmaceutics*, **11**, 493–512.
- Shirwaikar A., Issac D. and Malini S. (2004). Effect of *Aerva lanata* on cisplatin and gentamicin models of acute renal failure. *Journal of Ethnopharmacology*, **90**, 81–86.
- Sih-Sian L. and Yan-Kuin S. (2019). Improvement of the performance in Cr-doped ZnO memory devices via control of oxygen defects. *RSC Advance*, **9**, 2941–2947.
- Suresh Kumar C., Dhanaraj K., Vimalathithan R.M., Ilaiyaraja P. and Suresh G. (2021). Structural, Morphological and anti-bacterial analysis of nanohydroxyapatite derived from biogenic (SHELL) and chemical source: formation of apatite. *Iranian Journal of Materials Science and Engineering*, **18**, 91–109.
- Suresh Kumar C., Dhanaraj K., Vimalathithan R.M., Ilaiyaraja P. and Suresh G. (2021). Hydroxyapatite for bone related applications derived from seashell waste by simple precipitation method. *Journal of Asian Ceramic Societies*, **8**, 416–429.
- Tayyab Noman M., Amor N., Petru M., Mahmood A. and Kejzlar P. (2021). Photocatalytic Behaviour of Zinc Oxide Nanostructures on Surface Activation of Polymeric Fibres. *Polymers*. 13,1227–1245.
- Tee S.Y., Ye E., Pan P.H., Lee C.J., Hui H.K., Zhang S.Y., Koh L.D., Dong Z. and Han M.Y. (2015). Fabrication of bimetallic Cu/Au nanotubes and their sensitive, selective, reproducible and reusable electrochemical sensing of glucose. *Nanoscale*, **7**, 11190–11198.
- Teng C.P., Zhou T., Ye E., Liu S., Koh L.D., Low M., Loh X.J., Win K.Y., Zhang L. and Han M.Y. (2016). Effective Targeted Photothermal Ablation of Multidrug Resistant Bacteria and their Biofilms with NIR-Absorbing Gold Nanocrosses. *Advanced Healthcare Materials*, **5**, 2122–2130.
- Vishnukumar P., Vivekanandhan S., Misra M. and Mohanty A.K. (2018). Recent advances and emerging opportunities in phytochemical synthesis of ZnO nanostructures. *Materials Science in Semiconductor Processing*, **80**, 143–161.
- Vetrichelvan T. and Jegadeesan M. (2002). Anti-diabetic activity of alcoholic extract of *Aerva lanata* (L.) Juss. ex Schultes in rats. *Journal of Ethnopharmacology*, **80**, 103–107.
- Zhang Z., Shao C., Fei Gao., Li X. and Liu Y. (2010). Enhanced ultraviolet emission from highly dispersed ZnO quantum dots embedded in poly (vinyl pyrrolidone) electrospun nanofibers. *Journal of Colloidal Interface Sciences*, **347**, 215–220.